IOPscience iopscience.iop.org

Home Search Collections Journals About Contact us My IOPscience

Precision Measurement of Sub-50 nm Linewidth by Stitching Double-Tilt Images

This content has been downloaded from IOPscience. Please scroll down to see the full text.

2010 Jpn. J. Appl. Phys. 49 06GK06

(http://iopscience.iop.org/1347-4065/49/6S/06GK06)

View the table of contents for this issue, or go to the journal homepage for more

Download details:

IP Address: 140.113.38.11
This content was downloaded on 25/04/2014 at 06:21

Please note that terms and conditions apply.

Precision Measurement of Sub-50 nm Linewidth by Stitching Double-Tilt Images

Shan-Peng Pan[1,2], Huay-Chung Liou[1], Chao-Chang A. Chen[3], Jr-Rung Chen[3], and Tzong-Shi Liu[2]*

[1] *Center for Measurement Standards, Industrial Technology Research Institute, Hsinchu 30011, Taiwan*
[2] *Department of Mechanical Engineering, National Chiao Tung University, Hsinchu 30010, Taiwan*
[3] *Department of Mechanical Engineering, National Taiwan University of Science and Technology, Taipei 106, Taiwan*

Received November 30, 2009; accepted February 23, 2010; published online June 21, 2010

In this paper we present a stitching double-tilt image method (SDTIM) to measure sub-50 nm linewidth and to evaluate the measurement uncertainty. The SDTIM employs a parallel image method using a tilt mechanism to obtain two side scans. Moreover, the stitching method is used for linewidth determination. Experiments were performed by atomic force microscopy (AFM) using an ultrasharp tip, whose radius is smaller than 5 nm. The sample rotation axis is set parallel to the top surface of the sample in order to reduce the problem of measurement position variation. Experimental results show that the developed SDTIM can be used with an uncertainty of less than 5 nm at a confidence level of 95%.
© 2010 The Japan Society of Applied Physics

DOI: 10.1143/JJAP.49.06GK06

1. Introduction

The critical dimension (CD) is decreasing rapidly in semiconductor fabrication as a result of industrial demand. In order to avoid measurement of the doublet and to support the specifications for submicron features, advanced standard laboratories in many countries are attempting to develop traceable measurement systems based on the present standards. Accurate CD determination is difficult to achieve by CD scanning electron microscopy (CD-SEM) and conventional atomic force microscopy (AFM).[1] The specimen is prone to being burnt under the high electric current used in CD-SEM. Using conventional AFM, tip dilation is one of the problems encountered for CD measurement. It is important to set CD standards for the linewidth, sidewall angle (SWA), line edge roughness (LER), and linewidth roughness (LWR) on a nanometer scale for further semiconductor development. Many researchers have attempted to develop a new system or method for CD measurements. Murayama *et al.*[2] applied the tilt-scanning method to obtain a side profile. Zhao *et al.*[3] at the National Institute of Standards and Technology (NIST), USA, used a tilted nanotube tip to measure sidewall morphology and a sample rotation method to obtain two sidewall profiles for rotations of 0° and 180°. The actual profile was obtained by image stitching, but it may be difficult to find a same measuring region for the method of 180° sample rotation, especially when measuring a periodic pattern down to 50 nm. Orji and Dixson,[4] who also work at NIST, used a CD-AFM instrument with a boot-shaped tip to measure a sub 100 nm linewidth. However, the high cost of this sophisticated CD-AFM system restricts its applicability. In this study we developed a stitching double-tilt image method (SDTIM) to measure the linewidth and to evaluate the uncertainty in sub-50 nm linewidth measurements.

2. Measurement Procedure

Villarrubia[5] combined the morphology with set theory to simulate a scanning image and reconstruct a tip profile. Image dilation caused by a tip profile can be described by

$$I = S \oplus P, \tag{1}$$

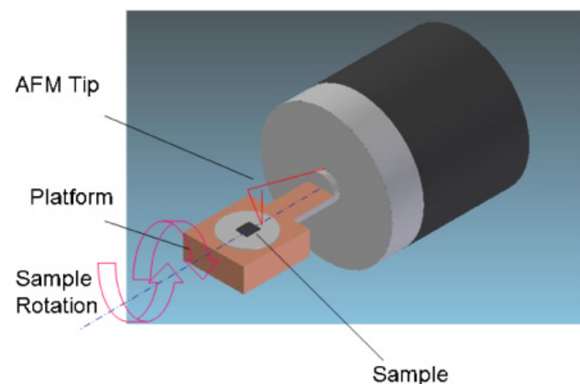

Fig. 1. (Color online) Scheme of tilt mechanism.

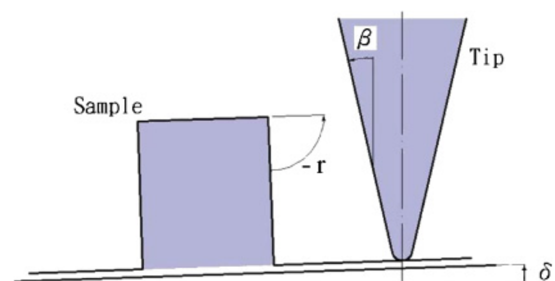

Fig. 2. (Color online) Relationship between tilted angle and half-conical angle.

where P denotes the probe set, S is the sample set, and I is the image set. In this paper we apply the parallel image method[6] to develop the SDTIM and to solve the image dilation problem. The parallel image method is conducted by using a tilt mechanism as shown in Fig. 1. The rotation axis is set parallel to the top surface of the sample to reduce the problem of shifting measuring position. A parallel image means that the periodic feature of on the sample is tilted and parallel to the axis of rotation. When the sample is tilted with a certain angle, the neighboring region can be measured, where δ is the tilted angle, β is the half-conical angle, and r denotes the sidewall angle relative the top plane. The relationship between the tilted angle and the half-conical angle is shown in Fig. 2. For example, one scan can be taken of a sample tilted to measure the linewidth, and then the sample can be tilted counterclockwise and measured again.

*E-mail address: tsliu@mail.nctu.edu.tw

 © 2010 The Japan Society of Applied Physics

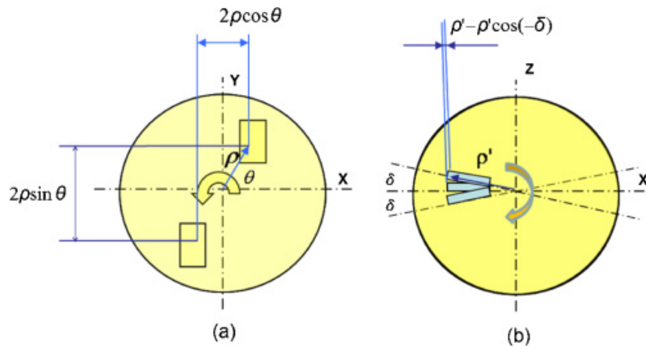

Fig. 3. (Color online) Demonstration of measuring-position shift for two methods: (a) in the X- and Z-directions for the rotating sample method and (b) in the Z-direction for the tilting-sample method.

Then, both images are stitched using the stitching procedure to generate an undistorted image.

The parallel image method is different from Zhao *et al.*'s method of rotating the sample by 180° method.[3] As shown in Fig. 3, ρ is the distance from the rotation center to the measuring position. Zhao *et al.*'s rotating sample method has the problem of a shift in his measuring position as shown in Fig. 3(a).

However, the shift position is small by the double-tilt sample method as shown in Fig. 3(b). In the experiments used to investigate the target was moved 37 µm along the horizontal axis and the tilted angle δ was 7°. Therefore, the distance ρ is given by $37\,\mu\text{m}/\sin 7° = 300\,\mu\text{m}$.

A commonly used method for stitching two images is the iterative closest point (ICP) algorithm.[3] A quaternion method[7] based on the ICP algorithm is used to determine the stitching results, and provides a standard for the evaluating the stitching results used to obtain the rotation and translation matrices with six degrees of freedom between the relative positions of the two images. This method handles six degrees of freedom and converges by using the least-mean-squares method. For the stitching procedure of two parallel images, the algorithm to obtain the rotation and translation matrices is described below.

a. Take two sets of data points from the different coordinate systems. The objective of registration is to transform the two sets of points into a common coordinate system. The centroids of the two sets of points, $F(f_1, f_2, \ldots, f_n)$ from image A and $S(s_1, s_2, \ldots, s_n)$ from image B, are calculated by

$$C_\text{f} = \frac{1}{n}\sum_{i=n}^{n} f_i \text{ and } C_\text{s} = \frac{1}{n}\sum_{i=n}^{n} s_i.$$

b. Calculate the new sets of points relative to the centroids: $P_i = f_i - C_\text{f}$ and $Q_i = s_i - C_\text{s}$.

c. Find the cross covariance matrix J of $\{P_i\}$ and $\{Q_i\}$: $J = \sum_{i=n}^{N} P_i Q_i^\text{T}$.

d. Construct J to obtain the following symmetric 4×4 matrix:

$$J_{4\times4} = \begin{bmatrix} J_{11}+J_{22}+J_{33} & J_{32}-J_{23} & J_{13}-J_{31} & J_{21}-J_{12} \\ J_{32}-J_{23} & J_{11}-J_{22}-J_{33} & J_{12}+J_{21} & J_{31}+J_{13} \\ J_{13}-J_{31} & J_{12}+J_{21} & -J_{11}+J_{22}-J_{33} & J_{23}+J_{32} \\ J_{21}-J_{12} & J_{31}+J_{13} & J_{23}+J_{32} & -J_{11}-J_{22}+J_{33} \end{bmatrix}, \quad (2)$$

and calculate the unit eigenvector q of $J_{4\times4}$: $q = [q_0\ q_1\ q_2\ q_3]^\text{T}$.

e. Write the rotation and translation matrices as follows:

$$R = \begin{bmatrix} q_0^2+q_1^2-q_2^2-q_3^2 & 2(q_1q_2-q_0q_3) & 2(q_1q_3+q_0q_2) \\ 2(q_1q_2+q_0q_3) & q_0^2+q_2^2-q_1^2-q_3^2 & 2(q_2q_3-q_0q_1) \\ 2(q_1q_3-q_0q_2) & 2(q_2q_3+q_0q_1) & q_0^2+q_3^2-q_1^2-q_2^2 \end{bmatrix} \quad (3)$$

$$T_\text{e} = C_\text{s} - RC_\text{f}. \quad (4)$$

f. The stitching parameters are determined by using the profile near the top and bottom edges. Image data on the sidewall are not used because they would adversely affect the accuracy of parameter determination. Considering two stitching images to be the maximum linewidth overlap after a horizontal translation T_s, the stitched image can be represented as

$$\text{Stitched image} = RC_\text{f} + T_\text{e} + T_\text{s}. \quad (5)$$

g. As shown in Fig. 4, a cross section of the image is obtained from the section E–E in Fig. 5. The value of the linewidth before tip diameter compensation can be determined from the distance between the fitting line y_b along the bottom of the cross section and the fitting line y_er, y_el of the two side edges at a feature with a certain height on the linewidth sample.

After compensate for the tip diameter, the linewidth can be determined from the stitched image. Considering the cosine angle error, shown in Fig. 6, where α is the coefficient of thermal expansion, ΔT is the temperature deviation, and ε is an error term including the tip diameter compensation, the linewidth can be written as

$$\text{LW} = \text{LW}_m \cos\theta(1 + \alpha\Delta T) + \varepsilon. \quad (6)$$

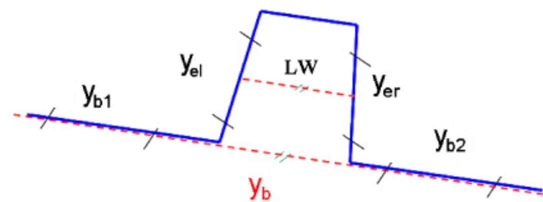

Fig. 4. (Color online) Scheme of a multiline fitting for linewidth calculation.

© 2010 The Japan Society of Applied Physics

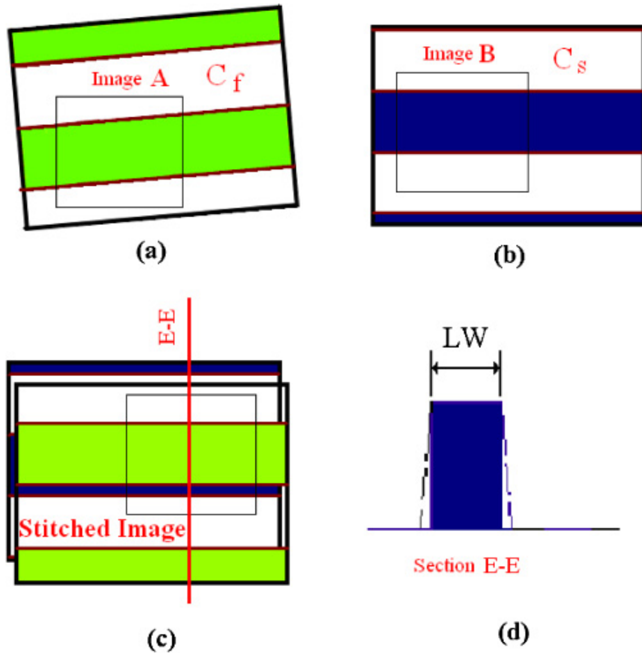

Fig. 5. (Color online) Scheme used for stitching two tilt images: (a) image A (b) image B (c) image created after stitching images A and B, and (d) cross section of stitched image.

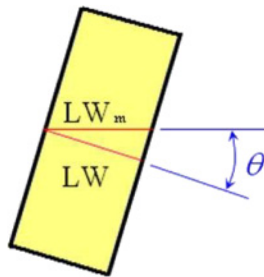

Fig. 6. (Color online) Scheme of the cosine error.

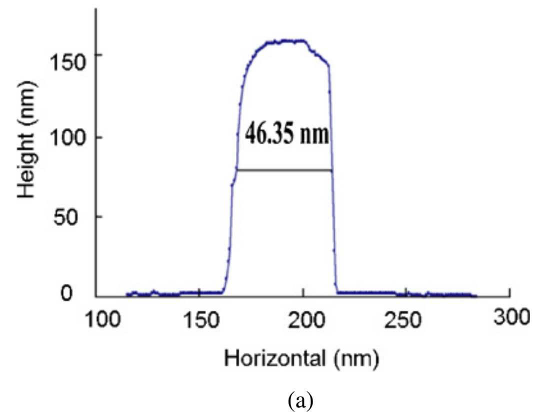

(a)

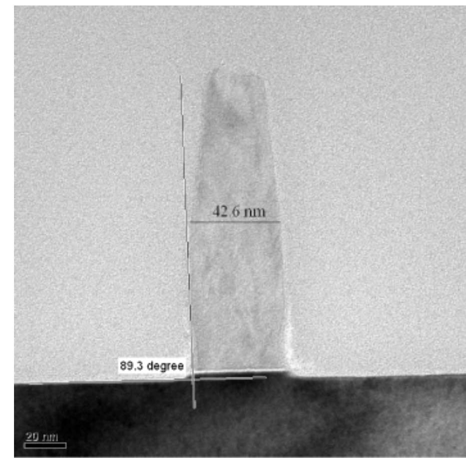

(b)

Fig. 7. (Color online) Stitching result compared with TEM image. (a) Experimental stitching result before tip diameter compensation at a height of 73.4 nm, and (b) TEM image of sample cross section.

3. Uncertainty Evaluation

3.1 Budget table of uncertainty

Linewidth measurements were performed using a Digital Instruments 3100 AFM apparatus and an Nanosensors SSS-NCHR AFM tip. The nominal diameter of the SSS-NCHR AFM tip was below 5 nm, and the nominal full-tip cone angle was 10°. The measured CD value before the compensation for the tip diameter was found to be 46.35 nm at a height of 73.4 nm, as shown in Fig. 7(a). The tip diameter was computed to be 6.23 nm using the scanning probe image processor (SPIP) software; this value was used to estimate the CD value as 40.12 nm. The comparison of this result with that obtained from the transmission electron microscopy (TEM) image shown in Fig. 7(b) revealed that the linewidth was 42.6 nm. Table I is a table of uncertainty budget in linewidth measurement, wherein the type-A evaluation of standard uncertainty is based on any valid statistical method for treating data, and the type-B evaluation of standard uncertainty is based on scientific judgment using all the available relevant information.[8)]

Referring to the ISO/IEC Guide 98-3: 2008,[9)] the procedure for estimating the uncertainty $u_c(\mathrm{LW})$ is based on the formula

Table I. Table of uncertainty budget in linewidth measurement.

Sources of uncertainty	Standard uncertainty component	Type
1. Linewidth measurement	LW_m	
(i) Repeatability	$u(\mathrm{LW}_{m1})$	A
(j) Resolution	$u(\mathrm{LW}_{m2})$	B
(k) Instrument accuracy	$u(\mathrm{LW}_{m3})$	B
2. Thermal expansion	α	
3. Deviation in the linewidth sample temperature	ΔT	B
4. Cosine error	θ	B
5. Uncertainty due to tip and software	ε	
(i) Approach of tip	$u(\varepsilon_1)$	B
(ii) Stylus tip wear	$u(\varepsilon_2)$	B
(iii) Stitching errors	$u(\varepsilon_3)$	A
(iv) Estimated radius of tip	$u(\varepsilon_4)$	B

$$u_c^2(\mathrm{LW}) = \left(\frac{\partial \mathrm{LW}}{\partial \mathrm{LW}_m}\right)^2 u^2(\mathrm{LW}_m) + \left(\frac{\partial \mathrm{LW}}{\partial \alpha}\right)^2 u^2(\alpha) + \left(\frac{\partial \mathrm{LW}}{\partial \Delta T}\right)^2 u^2(\Delta T) + \left(\frac{\partial \mathrm{LW}}{\partial \theta}\right)^2 u^2(\theta) + \left(\frac{\partial \mathrm{LW}}{\partial \varepsilon}\right)^2 u^2(\varepsilon) \quad (7)$$

with the following sensitivity coefficients:

© 2010 The Japan Society of Applied Physics

$$\frac{\partial \mathrm{LW}}{\partial \mathrm{LW}_m} = (1 + \alpha \Delta T)\cos\theta, \quad (8)$$

$$\frac{\partial \mathrm{LW}}{\partial \alpha} = \mathrm{LW}_m \Delta T \cos\theta, \quad (9)$$

$$\frac{\partial \mathrm{LW}}{\partial \Delta T} = \mathrm{LW}_m \alpha \cos\theta, \quad (10)$$

$$\frac{\partial \mathrm{LW}}{\partial \theta} = \mathrm{LW}_m (1 + \alpha \Delta T)\sin\theta, \quad (11)$$

$$\frac{\partial \mathrm{LW}}{\partial \varepsilon} = 1, \quad (12)$$

where the average linewidth is set as $\mathrm{LW} = 50\,\mathrm{nm}$, the variance of temperature is $\Delta T = 1\,\mathrm{K}$, the variance of θ is $\pm 1^\circ$, and the thermal coefficient of silicon is $\alpha = 2.55 \times 10^{-6}\,\mathrm{K}^{-1}$.

3.2 Sources of uncertainty $u(\mathrm{LW}_m)$

The sources of uncertainty in linewidth measurement include repeatability, resolution, and instrument accuracy.

3.2.1 Repeatability $u(\mathrm{LW}_{m1})$

In this study, for a linewidth of 50 nm, the repeatability error of the system is calculated form the 10 times measurement results. The standard deviation is denoted as $s(\mathrm{LW}_i)$, and is equal to 2.12 nm; the standard uncertainty obtained from this standard deviation is given as

$$u(\mathrm{LW}_{m1}) = \frac{2.12\,\mathrm{nm}}{\sqrt{10}} = 0.67\,\mathrm{nm}.$$

3.2.2 Resolution $u(\mathrm{LW}_{m2})$

The resolution depends on the measuring range and the data points. Assuming a rectangular distribution,[8] this component of the combined standard uncertainty is

$$u(\mathrm{LW}_{m2}) = \frac{\mathrm{Resoution}}{2\sqrt{3}}.$$

Table II summarizes the significant contributors to the uncertainty of resolution $u(\mathrm{LW}_{m2})$.

3.2.3 Instrument accuracy $u(\mathrm{LW}_{m3})$

According to the DI instrument specifications, the measuring errors are typically about $\pm 1\%$. We also calibrate the accuracy for the experimental instrument using a pitch standard gauge with 292 nm pitch. The pitch is calibrated by a diffractometer.[10] If $\mathrm{LW}_m = 50\,\mathrm{nm}$, the mean deviation of linewidth can be represented as $\pm 50\,\mathrm{nm} \times 1\%$. Assuming a rectangular distribution, this component of the combined standard uncertainty is $u(\mathrm{LW}_{m3}) = (50\,\mathrm{nm})(1\%)/\sqrt{3} = 0.29\,\mathrm{nm}$. Table III summarizes the significant contributors to the uncertainty of accuracy $u(\mathrm{LW}_{m3})$.

The square root of the sum of the squares of each standard uncertainty is $u(\mathrm{LW}_m) = [u^2(\mathrm{LW}_{m1}) + u^2(\mathrm{LW}_{m2}) + u^2(\mathrm{LW}_{m3})]^{1/2} = 0.79\,\mathrm{nm}$. The sensitivity coefficient is $\partial \mathrm{LW}/\partial \mathrm{LW}_m = (1 + \alpha\Delta T)\cos\theta = [1 + (2.25 \times 10^{-6}\,\mathrm{K}^{-1})(2.5\,\mathrm{K})] \cdot \cos(1^\circ) = 1$, and the component of combined standard uncertainty is $|\partial \mathrm{LW}_m/\partial \mathrm{LW}_m| u(\mathrm{LW}_m) = 0.79\,\mathrm{nm}$.

3.3 Uncertainty of thermal expansion α

The difference between the coefficients of thermal expansion for the sample and the linewidth sample is $1 \times 10^{-6}\,\mathrm{K}^{-1}$. Assuming a rectangular distribution, the uncertainty of the coefficient of thermal expansion is $u(\alpha) = 1.00 \times 10^{-6}\,\mathrm{K}^{-1}/\sqrt{3} = 5.17 \times 10^{-7}\,\mathrm{K}^{-1}$, and the sensitivity coefficient $\partial \mathrm{LW}/\partial\alpha = \mathrm{LW}_m \Delta T \cos\theta$ (nm K) depends on the measuring range. Table IV summarizes the significant contributors to the uncertainty of thermal expansion $u(\alpha)$.

3.4 Uncertainty of temperature ΔT

The temperature deviation in the linewidth sample is within $\pm 1.0\,\mathrm{K}$. The standard uncertainty is $u(\Delta T) = 1.0\,\mathrm{K}/\sqrt{3}$ and the sensitivity coefficient $\partial \mathrm{LW}/\partial \Delta T = \mathrm{LW}_m \alpha \cos\theta$ depends on the measuring range. Assuming a rectangular distribution, this component of the combined standard uncertainty is $\partial \mathrm{LW}/\partial \Delta T\, u(\Delta T)$. Table V summarizes the significant contributors to the uncertainty of temperature deviation $u(\Delta T)$.

3.5 Uncertainty of cosine error θ

The deviation of the angle of the analyzing line in the developed program is within $\pm 1^\circ$. The standard uncertainty

Table II. Summary of the significant contributors to uncertainty of resolution (unit: nm).

LW	Measurement range	Resolution	Uncertainty
LW = 50	512	1	0.29
50 < LW ≦ 100	1024	2	0.58
100 < LW ≦ 200	1536	3	0.87
200 < LW ≦ 500	2048	4	1.15

LW: linewidth

Table III. Summary of the significant contributors to uncertainty of accuracy (unit: nm).

LW	Measurement range	Accuracy	Uncertainty
LW = 50	512	0.5	0.29
50 < LW ≦ 100	1024	1	0.58
100 < LW ≦ 200	1536	2	1.15
200 < LW ≦ 500	2048	5	2.89

LW: linewidth

Table IV. Uncertainty of thermal expansion for various linewidth (unit: nm).

LW	Measuement range	$\lvert\partial \mathrm{LW}/\partial\alpha\rvert u(\alpha)$
LW = 50	512	2.59×10^{-5}
50 < LW ≦ 100	1024	5.17×10^{-4}
100 < LW ≦ 200	1536	1.03×10^{-4}
200 < LW ≦ 500	2048	2.59×10^{-4}

LW: linewidth

Table V. Uncertainty of temperature deviation (unit: nm).

LW	Measurement range	$\lvert\partial \mathrm{LW}/\partial \Delta T\rvert u(\Delta T)$
LW = 50	512	7.36×10^{-5}
50 < LW ≦ 100	1024	1.47×10^{-4}
100 < LW ≦ 200	1536	2.94×10^{-4}
200 < LW ≦ 500	2048	7.36×10^{-4}

LW: linewidth

© 2010 The Japan Society of Applied Physics

Table VI. Uncertainty of cosine error for various linewidths (unit: nm).

LW	Measurement range	$\lvert\partial \mathrm{LW}/\partial\theta\rvert u(\theta)$
LW = 50	512	8.79×10^{-3}
50 < LW ≦ 100	1024	1.76×10^{-2}
100 < LW ≦ 200	1536	3.52×10^{-2}
200 < LW ≦ 500	2048	8.79×10^{-2}

LW: linewidth

Table VII. Uncertainty due to stylus tip wear for various linewidths (unit: nm).

LW	Measurement range	$u(\varepsilon 2)$
LW = 50	512	0.47
50 < LW ≦ 100	1024	0.95
100 < LW ≦ 200	1536	1.42
200 < LW ≦ 500	2048	1.89

LW: linewidth

is $u(\theta) = (1°)(\pi/180°)/\sqrt{3}$ and the sensitivity coefficient is $\partial\mathrm{LW}/\partial\theta = \mathrm{LW}_m(1+\alpha\Delta T)\sin\theta$. Assuming a rectangular distribution, this component of the combined standard uncertainty is $\partial\mathrm{LW}/\partial\theta \cdot u(\theta)$. Table VI summarizes the significant contributors to the uncertainty of the cosine error $u(\theta)$.

3.6 Uncertainty due to tip and software ε

3.6.1 Uncertainty due to approach of tip $u(\varepsilon_1)$

From Fig. 8, the linewidth increases by with the number of times the tip approaches the sample. We performed an experiment using a tip to measure two images, and the linewidth dilation obtained was $0.22 \times 2 = 0.44$ nm. Assuming a rectangular distribution, the standard uncertainty due to the approach of the tip is $u(\varepsilon_1) = 0.44/2\sqrt{3} = 0.13$ nm and the sensitivity coefficient is $\partial\mathrm{LW}/\partial\varepsilon_1 = 1$.

3.6.2 Uncertainty due to stylus tip wear $u(\varepsilon_2)$

We carried out an experiment in which the slow-scanning axis was disabled through the control panel to investigate stylus tip wear. From Fig. 9, the linewidth increases with increasing scanning length. In the experiment we used a tip to obtain an image of 0.512 µm × 128 lines. The scanning included forward and backward motions, thus the linewidth dilation (y) was equal to $0.0125 \times (0.512 \times 128) \times 2 = 1.64$ nm. Assuming a rectangular distribution, the standard uncertainty due to stylus tip wear is $u(\varepsilon_2) = y/2\sqrt{3}$, and the sensitivity coefficient is $\partial\mathrm{LW}/\partial\varepsilon_2 = 1$. Table VII summarizes the significant contributors to the uncertainty due to tip wear $u(\varepsilon_2)$.

3.6.3 Uncertainty due to stitching errors $u(\varepsilon_3)$

The double-tilt images were stitched by using the ICP process, which converges to the local minimum value of a merit function. It is difficult to estimate the standard uncertainty of the ICP process on the basis of its formulation. The ICP process is assumed to be a black-box model. The standard uncertainty is evaluated on the basis of the relationship between the input and output values of the ICP process, which includes tilted and shifted images at different regions of two images. In this study, the stitching program

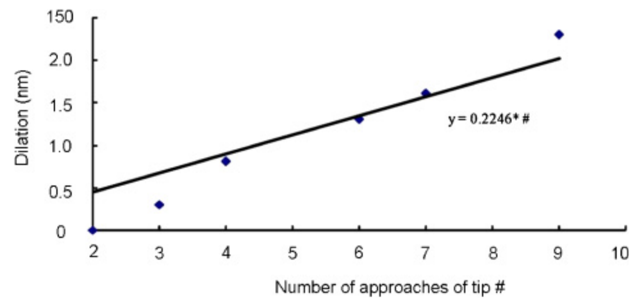

Fig. 8. (Color online) Relationship between numbers of approaches of tip and dilation.

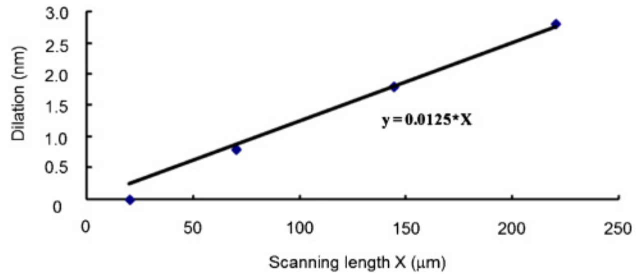

Fig. 9. (Color online) Relationship between scanning length and dilation.

calculates the same images but not the same selected stitching region 10 times. The standard uncertainty of the ICP process due to the stitching errors was obtained from the standard deviation of 10 times results as $u(\varepsilon_3) = 0.65$ nm for the different selected regions.

3.6.4 Uncertainty due to estimated radius of tip $u(\varepsilon_4)$

In the experiment we used an SSS-NCHR AFM tip with a radius smaller than 5 nm. Three images were separately measured using a new tip for each measurement. Each tip was reconstructed by measuring a nominal 45 nm NanoCD standard gauge with a rectangular profile (VLSI Inc.), and the tip size was estimated on the basis of the difference between the measured result at the top edge and the standard linewidth value, i.e., $P = I \Theta S$, derived from eq. (1). The linewidth was confirmed using TEM and was consistent with the National Institute of Standards and Technology (NIST) and the International System of Units (SI) on the basis of the atomic lattice spacing in single-crystal silicon. The reconstructed tip diameters obtained from the images and the three new tips are 6.9, 7.7, and 4.1 nm (average mean value 6.23 nm, standard deviation 1.9 nm); these values were verified by the TEM image shown in Fig. 10. The standard uncertainty is given by $u(\varepsilon_4) = 1.9/\sqrt{3} = 1.10$ nm, and the sensitivity coefficient is $\partial\mathrm{LW}/\partial\varepsilon_4 = 1$.

The square root of the sum of squares of each standard uncertainty is $u(\varepsilon) = [u^2(\varepsilon_1) + u^2(\varepsilon_2) + u^2(\varepsilon_3) + u^2(\varepsilon_4)]^{1/2} = 1.37$ nm. The sensitivity coefficient is $\partial\mathrm{LW}/\partial\varepsilon = 1$ and the combined uncertainty in this term is $\partial\mathrm{LW}/\partial\varepsilon \cdot u(\varepsilon) = 1.37$ nm.

3.7 Expanded uncertainty

According to ISO GUM,[9] the expanded uncertainty for a 50 nm linewidth is obtained from eq. (7) as

© 2010 The Japan Society of Applied Physics

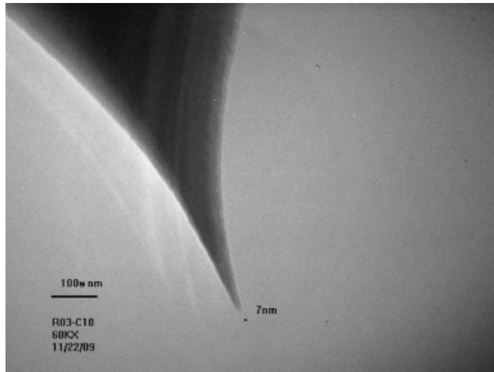

Fig. 10. TEM image of SSS-NCHR tip.

Table VIII. Expanded uncertainty of measured linewidths.

LW	u_c (nm)	k	U_{BMC} (nm)
LW = 50	1.57	2.0	3.2
50 < LW ≦ 100	1.92	2.0	3.9
100 < LW ≦ 200	2.48	2.0	5.0
200 < LW ≦ 500	3.89	2.0	7.8

LW: linewidth

$$u_c = [(0.79)^2 + (5.2 \times 10^{-5})^2 + (1.5 \times 10^{-4})^2 + (1.8 \times 10^{-2})^2 + (1.36)^2]^{1/2} = 1.57.$$

Finally, we calculate the expanded uncertainty $U = k \times u_c$[7] using measured linewidth, as shown in Table VIII, with a confidence level of 95%.

4. Results and Discussion

The stitching method utilized in this study involves the use of horizontal translation, different from conventional stitching methods. However, the use of this stitching method resulted in reduction of the major uncertainty components in the tip geometry and software to only 1.37 nm. In contrast, Zhao *et al.*[3] used nanotube tips to image samples; the uncertainties observed in the stitching results were approximately 30 nm for 1 μm linewidth measurement. Although our results were obtained using different samples, these results can be compared with each other because the scale of the calibration procedure during the pitch calibration in AFM was the same. The experimental results show that the SDTIM is superior to the method of Zhao *et al.*[3] This is because there are only two directions of measurement using the ultrasharp SSS-NCHR AFM tip. The ultrasharp tip provides a stable measuring state and excellent results for linewidth measurements using the SDTIM. Moreover, the expanded uncertainty also includes the 5 nm uncertainty observed in the sub-100-nm-linewidth measurement reported by Orji and Dixson;[4] in their study, a commercial instrument was used to perform the measurements at NIST and SEMATECH. Experimental results also showed that the measured linewidth was different from the specified value about 2–5 nm, which has been verified by TEM.

5. Conclusions

We developed the SDTIM method using an AFM instrument for CD measurements of sub 50 nm linewidth. Measurements were carried out for various three-dimensional nanoscale structures and to estimate the effect of the uncertainty factors on the CD values. The major components of uncertainty for the sub-50 nm linewidth measurements are listed in Table I. According to the experimental results, the tip diameter strongly affects the measured values for nanosize linewidths. Experimental results show that the developed method of linewidth measurement can be controlled with an uncertainty less than 5 nm and with a confidence level of 95%. This method can also be extended to the measurement of LER, LWR, and SWA. In future studies, a silicon crystal can be used as the standard for measuring the horizontal distance and vertical height to obtain an accuracy limit of 1 nm for length measurements in the sub-50 nm range.

1) C. G. Frase, E. Buhr, and K. Dirscherl: Meas. Sci. Technol. **18** (2007) 510.
2) K. Murayama, S. Gonda, H. Koyanagi, T. Terasawa, and S. Hosaka: Jpn. J. Appl. Phys. **45** (2006) 5423.
3) X. Zhao, J. Fu, W. Chu, C. Nguyen, and T. Vorburger: Proc. SPIE **5375** (2004) 363.
4) N. G. Orji and R. G. Dixson: Meas. Sci. Technol. **18** (2007) 448.
5) J. S. Villarubia: Surf. Sci. **321** (1994) 287.
6) C. C. A. Chen, J. R. Chen, H. C. L., and Y. L. Chen: Proc. 11th Int. Conf. Metrology and Properties of Engineering Surfaces, 2007, p. 281.
7) B. K. P. Horn: J. Opt. Soc. Am. A **4** (1987) 629.
8) B. N. Taylor and C. E. Kuyatt: NIST Technical Note 1297 (1994).
9) ISO/IEC Guide 98-3 (2008).
10) C. J. Chen, S. P. Pan, L. C. Chang, and G. S. Peng: Proc. SPIE **5190** (2003) 156.

 © 2010 The Japan Society of Applied Physics